Structural Engineering and Mechanics, Vol. 36, No. 5 (2010) 575-598
DOI: http://dx.doi.org/10.12989/sem.2010.36.5.575

Crack tip plastic zone under Mode I, Mode II and mixed mode (I+II) conditions

M.R. Ayatollahi* and Karo Sedighiani

Fatigue and Fracture Laboratory, Center of Excellence in Experimental Solid Mechanics and Dynamics, Department of Mechanical Engineering, Iran University of Science and Technology, Narmak, Tehran, 16846, Iran

(Received December 20, 2009, Accepted July 30, 2010)

Abstract. The shape and size of the plastic zone around the crack tip are analyzed under pure mode I, pure mode II and mixed mode (I+II) loading for small scale yielding and for both plane stress and plane strain conditions. A new analytical formulation is presented to determine the radius of the plastic zone in a non-dimensional form. In particular, the effect of *T*-stress on the plastic zone around the crack tip is studied. The results of this investigation indicate that the stress field with a *T*-stress always yields a larger plastic zone than the field without a *T*-stress. It is found that under predominantly mode I loading, the effect of a negative *T*-stress on the size of the plastic zone is more dramatic than a positive *T*-stress. However, when mode II portion of loading is dominating the effect of both positive and negative *T*-stresses on the size of the plastic zone is almost equal. For validating the analytical results, several finite element analyses were performed. It is shown that the results obtained by the proposed analytical formulation are in very good agreements with those obtained from the finite element analyses.

Keywords: plastic zone; crack; mixed mode (I+II); *T*-stress; analytical method.

1. Introduction

Theoretically, the linear elastic stress analysis of sharp cracks predicts infinite stresses at the crack tip. In fact, inelastic deformation, such as plasticity in metals and crazing in polymers, leads to relaxation of crack tip stresses caused by the yielding phenomenon at the crack tip. As a result, a plastic zone containing microstructural defects is formed. Consequently, the local stresses are limited to the yield strength of the material. The size and shape of the plastic zone can be estimated when moderate crack tip yielding occurs. The investigation of this plastic zone will not only help to predict the crack propagation angle under mixed mode loading (Khan and Khraisheh 2004, Bian and Kim 2004, Bian 2007), but also guide the engineering practices, such as crack prevention in design and manufacturing processes, and the arrest of crack extension in service. Therefore, an accurate description of the plastic zone is a key issue in the analysis of fracture events in engineering structures like defected pressure vessels and pipes.

The computation of the size and shape of the plastic zone depends on both loads and the state of

*Corresponding author, Professor, E-mail: m.ayat@iust.ac.ir

the stresses. Great efforts have been devoted to investigate the plastic zone around the crack tip on the basis of the classical criteria of elasticity or by calculations using the finite element method (e.g., Irwin 1949, Mishra and Parida 1985, Harmain and Provan 1997, Yuan and Broeks 1998, Kim *et al*. 2001, Jing *et al*. 2003, Khan and Khraisheh 2004, Bian and Kim 2004, Jing and Khraishi 2004, Benrahou *et al*. 2007). In mode I, Irwin (1949) assumed that the plastic zone is of a circular shape and computed its dimension in front of the crack r_y as

$$r_y = \frac{1}{\beta\pi}\left(\frac{K_I}{\sigma_{YS}}\right)^2 \tag{1}$$

where σ_{YS} is the yield stress, $\beta = 2$ for plane stress and $\beta = 6$ for plane strain. However the shape of the plastic zone predicted by Irwin is different from the actual one. Using a non-dimensional form of the radius as defined by the Mises yield criterion, Broek (1982) and Anderson (1995) have also presented some models for the shape and size of the plastic zone. Banks and Garlick (1984) and Zhang and Venugopalan (1987) investigated some factors which influence the shape and size of the plastic zone in the vicinity of the mode I crack in isotropic materials under small loads. Jing *et al*. (2003) predicted analytically the mode II plastic zone boundary for plane stress and plane strain conditions using the Mises and Tresca yield criteria. Khan and Khraisheh (2004) considered the shape and size of the mixed mode crack tip plastic zone for the case of an infinite plate with an inclined central crack under different loading conditions and they presented a new non-dimensional variable for the radius of plastic zone. However, these studies were based on the assumption that the fracture processes that occur close to the crack tip are dominated by the singular term alone in the Williams' (1957) expansion.

The stresses inside the plastic zone are influenced significantly by a remote *T*-stress. Thus, ignoring the *T*-stress can introduce considerable inaccuracies in studying of fracture. For example, Larsson and Carlsson (1973) have found that for the same values of K_I, the sign and magnitude of *T*-stress substantially change the shape and size of the crack tip plastic zone. Rice (1974) also used an analytical method and showed that the size of plastic zone around the crack tip is influenced by *T*. Detailed analyses for the structure of elastic-plastic stress fields around cracks were performed by Edmunds and Willis (1977) and Bilby *et al.* (1986) by employing the modified boundary layer formulation as suggested by Larsson and Carlsson (1973).

Later, Betegon and Hancock (1991) and Du and Hancock (1991) used finite element analysis to study the effects that different *T*-stress levels had on the near tip stress fields. They showed that negative *T*-stresses significantly lowered the crack tip constraint and caused the plastic zone to elongate and rotate forward. Conversely, positive *T*-stresses caused the plastic zone to contract and rotate backward.

Although there have been a wide range of studies on the effect of *T*-stress on the size and shape of the plastic zone, but in most cases these studies are confined only to mode I problems and very limited results are available for mode II and mixed mode (I+II) loading. Ayatollahi *et al*. (2002b) used the modified boundary layer formulation to investigate the effect of *T*-stress on the shape and size of the plastic zone for a mode II crack. They have shown that a positive *T* causes the direction of $r_{P\max}$ (the maximum radius of the plastic zone) to rotate clockwise. The lower section of the plastic zone behind the crack tip is also enlarged by a positive *T* whereas the upper section is contracted. Moreover, they have found that the effect of a negative *T*-stress on the shape of the plastic zone is the opposite of the effect for positive *T*. In similar study, Arun Roy and Narasimhan (1997) have shown that under mixed mode loading, an increase in the magnitude of a positive *T*-

stress from zero causes the top lobe of the plastic zone to vanish and the bottom lobe to expand along the crack face. On the contrary, a decrease in the magnitude of a negative *T*-stress causes the bottom lobe to vanish and the top lobe to extend ahead of the crack tip.

Finite element analysis has been traditionally recognized as the most general technique for evaluating the crack tip plastic zone for different modes of loading. However, a reliable finite element analysis often requires extensive computational time, expertise and resources, which make the computation quite expensive. This method has also to be carried out on a case-by-case basis for each component. Meanwhile, there is no exact analytical solution to estimate the plastic zone boundary for different loading and geometry conditions when the *T*-stress is present in the stress relations. Therefore, there is need to devise an exhaustive way for determining a normalized radius of the plastic zone applicable to various loading conditions.

The main propose of this paper is to investigate the influence of *T*-stress on the size and shape of the plastic zone ahead of mode I, mode II and mixed mode cracks tip for small to moderate scale yielding. In the present study, an analytical formulation for the normalized radius of the plastic zone is presented which can be used for different loading and geometrical conditions. The proposed formulation describes the effect of *T*-stress on the plastic zone boundary for both plane strain and plane stress conditions in a fairly straightforward way. In order to validate the presented non-dimensional formulation, several finite element analyses are performed. In this paper, the boundary layer model (BLM) (Haefele and Lee 1995) is used to study the effect of far field stresses on the size and shape of the plastic zone around the crack tip. The numerical results are in very good agreement with the analytical ones.

2. Analysis

2.1 Background

Brittle fracture is a major mode of failure in components and structures containing cracks. Crack growth in brittle materials often takes place very fast and with serious consequences. Therefore, it is important to define an appropriate procedure for predicting the onset of brittle fracture in cracked specimens. In linear elastic fracture mechanics (LEFM), the stress intensity factor, K, characterizes the magnitude of the stress field in the vicinity of a crack tip. It is also used to predict the onset of fracture.

This theory consideration still can be true for an elastic-plastic crack problem if the plastic zone size is small compared to other dimensions of the specimen, such as the crack length. This is the so-called 'small scale yielding approximation' by Rice (1968). Then the crack problem can be studied by assuming that the near tip stress field of the elastic-plastic crack problem is approximated by the singular term in the elastic stress solution of Williams' (1957) series expansion

$$\sigma_{ij} = Ar^{1/2}f_{ij}(\theta) + Br^{0}g_{ij}(\theta) + Cr^{1/2}h_{ij}(\theta) + \ldots \tag{2}$$

where r and θ are polar coordinates with the origin located at the crack tip (Fig. 1) and σ_{ij} denotes the stress tensor. The non-dimensional functions $f_{ij}(\theta)$, $g_{ij}(\theta)$ and $h_{ij}(\theta)$ describe the angular variation of the stress field. The parameters A, B and C are proportional to the applied load. As $r \rightarrow 0$, the leading term dominates and exhibits $r^{-1/2}$ singularity, while the higher order terms remain a finite value or approach zero. Therefore, the first singular term of the Williams expansion is dominant and

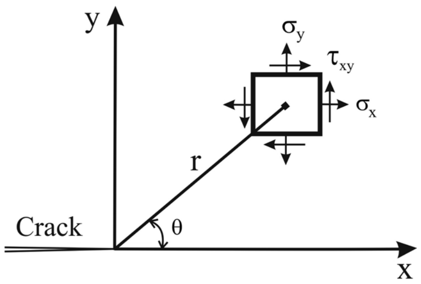

Fig. 1 Stresses at the crack tip

other terms are usually neglected. Over the recent years, an increasing attention has been devoted to study the effect of higher order terms of Williams' series expansion on the initiation of mode I fracture under the predominantly linear elastic deformation. Larsson and Carlsson (1973) investigated the elastic-plastic crack problem in different types of specimens using finite element method (FEM) and found that the solution for the stress state near the crack tip can not be related to Eq. (2) through the mode I stress intensity factor K_I alone, even when the requirements for 'small scale yielding' are all met. They noted that the discrepancies could be resolved if the first non-singular term of Williams' series expansion (see Eq. (3)) is included in the near tip stress solution, which is

$$\sigma_{ij} = \frac{K_I}{\sqrt{2\pi r}} f_{ij}(\theta) + T_{ij}\delta_{1i}\delta_{1j} \tag{3}$$

T_{11} represents a uniform stress acting parallel to the crack plane. In the notation of Rice (1974), this second term of Williams' series expansion is denoted as the *T*-stress or elastic *T*-stress. The *T*-stress is dependent on the loads applied to the cracked structure, crack length and overall geometrical parameters. Bilby *et al*. (1986) have shown that a two-parameter (T and K_I) remote loading approach characterizes the very near tip elastic-plastic fields of a non-hardening blunted crack better than does K_I alone. Al-Ani and Hancock (1991), Betegon and Hancock (1991), Du and Hancock (1991), O'Dowd and Shih (1991), and Wang (1993) performed further studies to investigate the elastic-plastic crack tip field using T in addition to the singular term and they showed that T can be used as a measure of the crack tip constraint in mode I.

Based on the classical definition for modes of crack deformation (Rice 1968), *T*-stress disappears for pure mode II loading. However, some analytical and numerical researches indicate that this term can also exist in mode II problems (e.g., Arun Roy and Narasimhan 1997, Ayatollahi *et al*. 1996, 1998, 2002a, b, Smith *et al*. 2001, Fett 2001), and ignoring its effect can introduce significant inaccuracies in predicting mode II fracture. Ayatollahi *et al*. (1996, 1998) have recently demonstrated that there are many real mode II loading conditions where significant values of T exist. Further, Ayatollahi *et al*. (2002b) have shown that the stresses inside the plastic zone are influenced significantly by a remote *T*-stress. Thus, ignoring the *T*-term in mode II can introduce considerable inaccuracies in studying mode II brittle fracture.

2.2 Pure mode I and mode II plastic zone

For an isotropic crack body under pure mode I or pure mode II conditions, the first two terms of stress fields around a crack tip can be written as

$$\sigma_x = \frac{K_i}{\sqrt{2\pi r}} f_{i1}(\theta) + T$$
$$\sigma_y = \frac{K_i}{\sqrt{2\pi r}} f_{i2}(\theta)$$
$$\tau_{xy} = \frac{K_i}{\sqrt{2\pi r}} f_{i3}(\theta) \qquad i = I \text{ or } II$$
$$\sigma_z = 0 \quad \textit{for plane stress}$$
$$\sigma_z = \nu(\sigma_x + \sigma_y) \quad \textit{for plane strain} \tag{4}$$

where υ is Poisson's ratio and the angular functions $f_{i1}(\theta)$, $f_{i2}(\theta)$ and $f_{i3}(\theta)$ are (Williams 1957)

$$f_{I1}(\theta) = \cos\frac{\theta}{2}\left(1 - \sin\frac{\theta}{2}\sin\frac{3\theta}{2}\right)$$
$$f_{I2}(\theta) = \cos\frac{\theta}{2}\left(1 + \sin\frac{\theta}{2}\sin\frac{3\theta}{2}\right)$$
$$f_{I3}(\theta) = \sin\frac{\theta}{2}\cos\frac{\theta}{2}\cos\frac{3\theta}{2} \tag{5a}$$

and

$$f_{II1}(\theta) = -\sin\frac{\theta}{2}\left(2 + \cos\frac{\theta}{2}\cos\frac{3\theta}{2}\right)$$
$$f_{II2}(\theta) = \sin\frac{\theta}{2}\cos\frac{\theta}{2}\cos\frac{3\theta}{2}$$
$$f_{II3}(\theta) = \cos\frac{\theta}{2}\left(1 - \sin\frac{\theta}{2}\sin\frac{3\theta}{2}\right) \tag{5b}$$

for mode I and mode II, Respectively. Once the stress field around the crack tip is defined, a yield criterion can be employed to determine the plastic zone around the crack tip. Here, the Von Mises yield function as

$$(\sigma_x - \sigma_y)^2 + (\sigma_x - \sigma_z)^2 + (\sigma_z - \sigma_y)^2 + 6\tau_{xy}^2 = 2\sigma_{YS}^2 \tag{6}$$

is used to predict the radius of the plastic zone, where σ_{YS} is the yield stress of the material. Upon substituting Eqs. (4) and (5) into the Mises yield criterion (Eq. (6)), a relation for the boundary of the plastic zone r_p can be calculated. This relation, however, depends on the loading condition through its dependence on K_I or K_{II} and T. To obtain a generalized radius for the plastic zone applicable to all loading conditions, we have to define a normalized radius. Using a non-dimensional form of the radius, Broek (1982) and Anderson (1995) showed the shape and size of the plastic zone for pure mode I, pure mode II, and pure mode III cases but for the particular case of $T = 0$. Therefore, in these studies the respective stress intensity factor is used to normalize the plastic zone radius. For example, for pure mode I, the normalized plastic zone radius for plane stress and plane strain conditions are written as Eqs. 7(a) and 7(b) (Broek 1982, Anderson 1995), respectively.

$$R_{PI}(\theta) = \frac{r_{PI}}{\frac{1}{2\pi}\left(\frac{K_I}{\sigma_{ys}}\right)^2} = \frac{1}{2}\left(1+\cos\theta+\frac{3}{2}\sin^2\theta\right) \tag{7a}$$

$$R_{PI}(\theta) = \frac{r_{PI}}{\frac{1}{2\pi}\left(\frac{K_I}{\sigma_{ys}}\right)^2} = \frac{1}{2}\left((1-2\nu)^2(1+\cos\theta)+\frac{3}{2}\sin^2\theta\right) \tag{7b}$$

where R_{PI} is the normalized mode I plastic zone radius. When the T-stress is ignored, only the stress intensity factor appears in the equations and is used to normalize the plastic zone radius. Therefore, it is important to devise a comprehensive way of presenting the normalized plastic zone radius when both K_I and T or K_{II} and T appear in the equations.

The substitution of the stress terms from Eqs. (4) and (5) into Eq. (6) and manipulating the resultant expressions yields

$$\begin{aligned}&\left(\frac{K_i}{\sqrt{2\pi r}}\right)^2[h(f_{i1}(\theta)+f_{i2}(\theta))^2+3(f_{i3}^2(\theta)-f_{i1}(\theta)f_{i2}(\theta))]\\&+\frac{K_i}{\sqrt{2\pi r}}T[2h(f_{i1}(\theta)+f_{i2}(\theta))-3f_{i2}(\theta)]+T^2h = \sigma_{YS}^2\end{aligned} \tag{8}$$

where h is 1 for plane stress and $(1-\upsilon+\upsilon^2)$ for plane strain. For more simplification $F_{i1}(\theta, \upsilon)$, $F_{i2}(\theta, \upsilon)$ and Q_i are defined as

$$\begin{aligned}F_{i1}(\theta,\nu) &= h(f_{i1}(\theta)+f_{i2}(\theta))^2+3(f_{i3}^2(\theta)-f_{i1}(\theta)f_{i2}(\theta))\\F_{i2}(\theta,\nu) &= 2h(f_{i1}(\theta)+f_{i2}(\theta))-3f_{i2}(\theta)\\Q_i &= \frac{K_i}{\sqrt{2\pi r}}\frac{1}{T}\end{aligned} \tag{9}$$

Substituting these functions into Eq. (8) gives

$$Q_i^2F_{i1}(\theta,\nu)+Q_iF_{i2}(\theta,\nu)+\left(h-\frac{1}{b^2}\right) = 0 \tag{10}$$

where b is the non-dimensional ratio T/σ_{YS}. Consequently, the solution of Eq. (10) for Q_i is obtained as

$$Q_i = \frac{-F_{i2}(\theta,\nu)\pm\sqrt{F_{i2}^2(\theta,\nu)-4F_{i1}(\theta,\nu)(h-1/b^2)}}{2F_{i1}(\theta,\nu)} \tag{11}$$

in the above equation the positive sign is used for positive T-stresses and the negative one is used for negative T-stresses. The normalized plastic zone radius is now defined as

$$R_{Pi} = \frac{r_{Pi}}{\frac{1}{2\pi}\left(\frac{K_i}{\sigma_{YS}}\right)^2} = \left(\frac{1}{bQ_i}\right)^2 \tag{12}$$

and Eq. (5) and Eq. (12) are replaced into Eq. (12), the normalized plastic zone radius R_p takes the following form

$$R_{PI} = \frac{r_{PI}}{\frac{1}{2\pi}\left(\frac{K_I}{\sigma_{YS}}\right)^2} =$$

$$\left(\frac{2\cos^2\left(\frac{\theta}{2}\right)(3-8h+3\cos\theta)}{b((7.5-8h)\cos\left(\frac{\theta}{2}\right)\pm\left(\cos^2\left(\frac{\theta}{2}\right)\left(8\left(\frac{1}{b^2}-h\right)(-3+8h-3\cos\theta)-(6-8h+3\cos\theta-3\cos(2\theta))^2\right)\right)^{0.5}-1.5\cos\left(\frac{5\theta}{2}\right)}\right)^2 \quad (13a)$$

for mode I, and

$$R_{PII} = \frac{r_{PII}}{\frac{1}{2\pi}\left(\frac{K_{II}}{\sigma_{YS}}\right)^2} =$$

$$\left(\frac{(3+16h-4(-3+4h)\cos\theta+9\cos2\theta)}{b(-3+16h)\sin\frac{\theta}{2}\pm2\left(2\left(\frac{1}{b^2}-h\right)(3+16h-4(-3+4h)\cos\theta+9\cos2\theta)+(8h+3\cos\theta+3\cos2\theta)^2\sin^2\frac{\theta}{2}\right)^{0.5}+3\sin\frac{5\theta}{2}}\right)^2 \quad (13b)$$

for mode II conditions. Eqs. 13(a) and 13(b) show two closed form solutions for the normalized plastic zone radius around a mode I and mode II crack tip which can be used for both plane stress and plane strain conditions. Again, the positive and negative signs in the denominator of these equations are used for positive and negative *T*-stresses, respectively. According to this equation, the normalized plastic zone radius is a function of angle θ and the non-dimensional parameter *b*. It is also a function of Poisson's ratio but only for plane strain conditions.

2.3 Analysis of the mixed mode (I+II) plastic zone

The stress components based on the first two terms of the mixed mode (I+II) elastic crack tip field can be written as

$$\begin{aligned}
\sigma_x &= \frac{K_I}{\sqrt{2\pi r}} f_{I1}(\theta) + \frac{K_{II}}{\sqrt{2\pi r}} f_{II1}(\theta) + T \\
\sigma_y &= \frac{K_I}{\sqrt{2\pi r}} f_{I2}(\theta) + \frac{K_{II}}{\sqrt{2\pi r}} f_{II2}(\theta) \\
\tau_{xy} &= \frac{K_I}{\sqrt{2\pi r}} f_{I3}(\theta) + \frac{K_{II}}{\sqrt{2\pi r}} f_{II3}(\theta)
\end{aligned} \quad (14)$$

where υ is Poisson's ratio and the angular functions $f_{i1}(\theta)$, $f_{i2}(\theta)$ and $f_{i3}(\theta)$ have been defined in Eqs. 5(a) and 5(b). In the case of pure mode I or pure mode II, either K_I or K_{II} is equal to zero, therefore to simplify the equations only K_I or K_{II} appears in the equations with *T*. However, for mixed mode condition K_I, K_{II} and *T* should be considered all together. Therefore, it is necessary to devise a comprehensive way of presenting the normalized plastic zone radius when K_I, K_{II} and *T* appear in the equations, simultaneously. In general, the stress intensity factors can be defined as:

$$K_i = \sigma_{app} Y_i \sqrt{\pi a} \qquad i = I \text{ or } II \tag{15}$$

where σ_{app} is the applied stress, and Y_I and Y_{II} are the mode I and mode II geometry factors, respectively. To evaluate the characteristics of mixed mode crack, it is necessary to introduce an effective stress intensity factor K_{eff} that considers the mode I and mode II stress intensity factors simultaneously. K_{eff} is often defined as

$$K_{eff} = \sqrt{K_I^2 + K_{II}^2} = \sigma_{app}\sqrt{\pi a}\sqrt{Y_I^2 + Y_{II}^2} \tag{16}$$

The substitution of the stress terms from Eqs. (5), (14) and (15) into Eq. (6) and manipulating the resultant expression yields

$$\left(\frac{\sigma_{app}\sqrt{\pi a}}{\sqrt{2\pi r}}\right)^2 [Y_I^2 F_1(\theta, \nu) + Y_{II}^2 G_1(\theta, \nu) + Y_I Y_{II} L_1(\theta, \nu)] + T\left(\frac{\sigma_{app}\sqrt{\pi a}}{\sqrt{2\pi r}}\right)[Y_I^2 F_2(\theta, \nu) + Y_{II}^2 G_2(\theta, \nu)] + T^2 = \sigma_{ys}^2 \tag{17}$$

In the above equation $F_1(\theta, \upsilon)$, $G_1(\theta, \upsilon)$, $L_1(\theta,\upsilon)$, $F_2(\theta,\upsilon)$ and $G_2(\theta,\upsilon)$ are defined as

$$\begin{aligned}
F_1(\theta, \nu) &= h(f_{I1}(\theta) + f_{I2}(\theta))^2 + 3(f_{I3}^2(\theta) - f_{I1}(\theta)f_{I2}(\theta)) \\
G_1(\theta, \nu) &= h(f_{II1}(\theta) + f_{II2}(\theta))^2 + 3(f_{II3}^2(\theta) - f_{II1}(\theta)f_{II2}(\theta)) \\
L_1(\theta, \nu) &= 3(-f_{I2}(\theta)f_{II1}(\theta) - f_{I1}(\theta)f_{II2}(\theta) + 2f_{I3}(\theta)f_{II3}(\theta)) \\
&\quad + 2h(f_{I1}(\theta)f_{II1}(\theta) + f_{I2}(\theta)f_{II1}(\theta) + f_{I1}(\theta)f_{II2}(\theta) + f_{I2}(\theta)f_{II2}(\theta)) \\
F_2(\theta, \nu) &= 2h(f_{I1}(\theta) + f_{I2}(\theta)) - 3f_{I2}(\theta) \\
G_2(\theta, \nu) &= 2h(f_{II1}(\theta) + f_{II2}(\theta)) - 3f_{II2}(\theta)
\end{aligned} \tag{18}$$

where h is 1 for plane stress and $(1 - \upsilon + \upsilon^2)$ for plane strain. For more simplification $F^1_{(I+II)}$ (θ, υ, Y), $F^2_{(I+II)}$ (θ, υ, Y), and $Q_{(I+II)}$ are defined as

$$F^1_{(I+II)}(\theta, \nu, Y) = Y_I^2 F_1(\theta, \nu) + Y_{II}^2 G_1(\theta, \nu) + Y_I Y_{II} L_1(\theta, \nu)$$

$$F^2_{(I+II)}(\theta, \nu, Y) = Y_I F_2(\theta, \nu) + Y_{II} G_2(\theta, \nu)$$

$$Q_{(I+II)} = \frac{1}{T}\left(\frac{\sigma_{app}\sqrt{\pi a}}{\sqrt{2\pi r}}\right) \tag{19}$$

Substituting these functions into Eq. (17) gives

$$Q^2_{(I+II)} F^1_{(I+II)}(\theta, \nu, Y) + Q_{(I+II)} F^2_{(I+II)}(\theta, \nu, Y) + \left(h - \frac{1}{b^2}\right) = 0 \tag{20}$$

where b is the non-dimensional ratio of the T-stress to the yield stress of the material. Consequently, the solution of Eq. (20) for Q is obtained as

$$Q_{(I+II)} = \frac{-F^2_{(I+II)}(\theta, \nu, Y) \pm \sqrt{(F^2_{(I+II)}(\theta, \nu, Y))^2 - 4F^1_{(I+II)}(\theta, \nu, Y)(h - 1/b^2)}}{2F^1_{(I+II)}(\theta, \nu, Y)} \tag{21}$$

The plastic zone radius for a mixed mode crack is defined as

$$r_{P(I+II)} = \frac{a}{2}\left(\frac{\sigma_{app}}{\sigma_{ys}}\right)^2\left(\frac{1}{bQ_{(I+II)}}\right)^2 \tag{22}$$

Consequently, by replacing Eqs. (5), (16) and (21) into Eq. (22), the normalized plastic zone radius $R_{P(I+II)}$ takes the following form for mixed mode (I+II) condition

$$R_{P(I+II)} = \frac{r_{P(I+II)}}{\frac{1}{2\pi}\left(\frac{K_{eff}}{\sigma_{YS}}\right)^2} = \frac{1}{1+R_K^2}\left(\frac{2\left(\frac{1}{b}\right)G^1_{(I+II)}}{G^2_{(I+II)} + \left(\frac{1}{2}(G^2_{(I+II)})^2 \pm 4\left(\frac{1}{b^2} - h\right)G^1_{(I+II)}\right)^{.5}}\right)^2 \tag{23}$$

where R_K is the non-dimensional ratio K_{II}/K_I. $G^1_{(I+II)}$ and $G^2_{(I+II)}$ are functions of θ, R_K and υ which are determined as

$$G^1_{(I+II)} = \frac{1}{8}\left(-4\cos^2\left(\frac{\theta}{2}\right)(3 - 8h + 3\cos\theta) + R_K^2(3 + 16h + (12 - 16h)\cos\theta + 9\cos 2\theta) + 8R_K(3 - 4h + 3\cos\theta)\sin\theta\right)$$

$$G^2_{(I+II)} = -\frac{1}{2}\cos\left(\frac{\theta}{2}\right)(-6 + 8h - 3\cos\theta + 3\cos 2\theta) + \frac{1}{2}R_K\sin\frac{\theta}{2}(8h + 3\cos\theta + 3\cos 2\theta) \tag{24}$$

Eq. (23) shows a closed form solution for the normalized plastic zone radius under mixed mode loading which can be used for both plane stress and plane strain conditions. The positive and negative signs in Eqs. (21) and (23) are used for positive and negative *T*-stresses, respectively. According to this equation, the normalized plastic zone radius is a function of the non-dimensional parameters θ, b and R_K. It is also a function of Poisson's ratio but only for plane strain conditions.

3. Linear elastic finite element analysis

In order to validate the presented non-dimensional formulation, a boundary layer model (Haefele and Lee 1995) was used to simulate crack tip region for different loading conditions. In BLM, the stresses or displacements corresponding to the first term of Williams' series solution are used as the far field boundary conditions. Larsson and Carlsson (1973) later modified the boundary layer model by adding the effect of *T*-stress, the constant second term in the Williams' solution. The finite element code ABAQUS V6.6-3 was used to analyze the boundary layer model. A circular region containing an edge crack was considered with the crack tip placed in the center of the circle. The finite element mesh for the boundary layer model of radius 200 mm is shown in Fig. 2 with 80 rings of elements, each consisting of 32 eight-noded quadrilateral elements in the circumferential direction from $-\pi$ through π. The density of nodal points was biased towards the crack tip such that the length of the elements in the first ring next to the crack tip was 5×10^{-6} times the radius of the

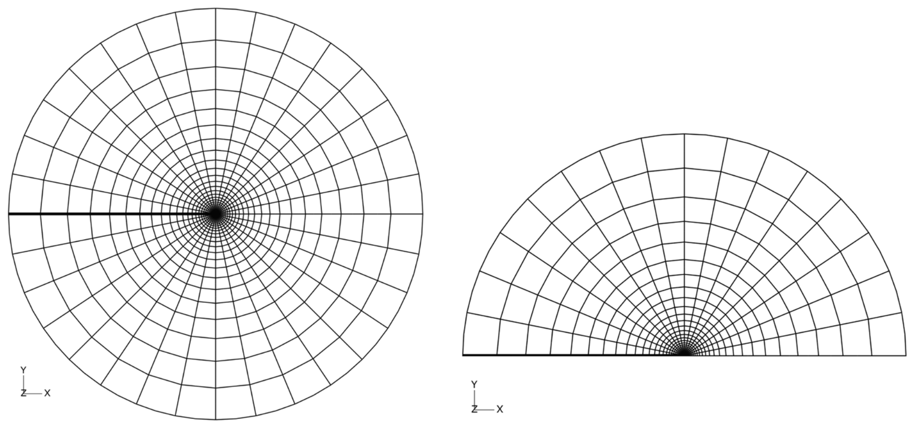

(a) (b)

Fig. 2 Finite element mesh for boundary layer model analysis (a) For mode II and mixed mode loading, (b) For mode I loading

boundary layer model (Fig. 2). Due to symmetry, the finite element calculations in the case of pure mode I were carried out using a semi-circular region of radius R_0 as shown in Fig. 2(b).

Young's modulus E, Poisson's ratio ν and the yield stress σ_{YS} were taken as 210 GPa, 0.3 and 400 MPa, respectively. Selected finite element calculations confirmed that the present model is able to reproduce the results of similar analyses reported by Ayatollahi *et al*. (2002b).

To comply with the requirements for small scale yielding, the loading conditions along the boundary were such chosen that the maximum radius for the plastic zone around the crack tip remained very small compared with the radius of the circle. The displacements corresponding to mode I, mode II and mixed mode fields were applied along the circular boundary. For mode I loading condition K_{II} is equal to zero, while for mode II loading condition K_I equals zero. The displacement components u_x and u_y can be calculated from the displacement field (Haefele and Lee 1995) as

$$u_x = \frac{(1+\nu)}{E}\sqrt{\frac{R_0}{2\pi}}\left\{K_I\cos\left(\frac{\theta}{2}\right)\left(\kappa-1+2\sin^2\left(\frac{\theta}{2}\right)\right)+K_{II}\sin\left(\frac{\theta}{2}\right)\left(\kappa+1+2\cos^2\left(\frac{\theta}{2}\right)\right)\right\}+T\frac{1-\nu^2}{E}R_0\cos\theta$$

$$u_y = \frac{(1+\nu)}{E}\sqrt{\frac{R_0}{2\pi}}\left\{K_I\sin\left(\frac{\theta}{2}\right)\left(\kappa+1-2\cos^2\left(\frac{\theta}{2}\right)\right)+K_{II}\cos\left(\frac{\theta}{2}\right)\left(\kappa-1-2\sin^2\left(\frac{\theta}{2}\right)\right)\right\}-T\frac{\upsilon(1+\nu)}{E}R_0\sin\theta \tag{25}$$

The bulk modulus κ is $(3-4\upsilon)$ and $(3-\upsilon)/(1+\upsilon)$ for plane strain and plane stress conditions, respectively. Since, Eq. (25) is based on the elastic stress distributions it is important that the boundary at which the displacements are applied is sufficiently far from the crack tip plastic zone, otherwise the elastic conditions defined at the boundary would be violated. In this paper, the Von Mises yield model in conjunction with a linear elastic analysis is used to calculate the plastic zone boundary.

4. Results and discussion

In this section the effect of *T*-stress on the shape and size of the plastic zone is studied using the analytical formulations proposed in the previous sections and the results are compared with those obtained from the finite element analysis. The present study considers three sets of analyses, $T > 0$, $T = 0$ and $T < 0$, to study the effect of *T*-stress on the shape and size of the plastic zone near the crack tip. The plastic zone represents the region where the effective stress σ_{eff} exceeds the yield stress σ_{YS}. It was found that in the case of elastic analysis, the plastic zone boundary for $|T/\sigma_{YS}| > 0.7$ extends towards the remote boundary. Since for $|T/\sigma_{YS}| > 0.7$, the maximum radius of the plastic zone becomes too large compared to the crack length a, and the requirements of small scale yielding conditions will be violated, the results are presented only for $|T/\sigma_{YS}| < 0.7$. Within this limit an extensive range of real crack specimens can still be simulated. Thirteen special values of the *T*-stress, i.e., $T/\sigma_{YS} = 0$, ± 0.1, ± 0.2, ± 0.33, ± 0.5, ± 0.57 and ± 0.67, are utilized in the analytical and elastic FE calculations. Before the discussion of the results, it is noted that all the plastic zone radii have been normalized with respect to $1/2\pi(K_{eff}/\sigma_{YS})^2$.

4.1 Mode I crack tip plastic zone

The plastic zone boundaries normalized with respect to $1/2\pi(K_I/\sigma_{YS})^2$ and calculated from both the proposed formulation and the finite element analyses are plotted in Fig. 3 for the selected values of T and under plane stress condition. Since in the case of mode I the plastic zone is symmetric

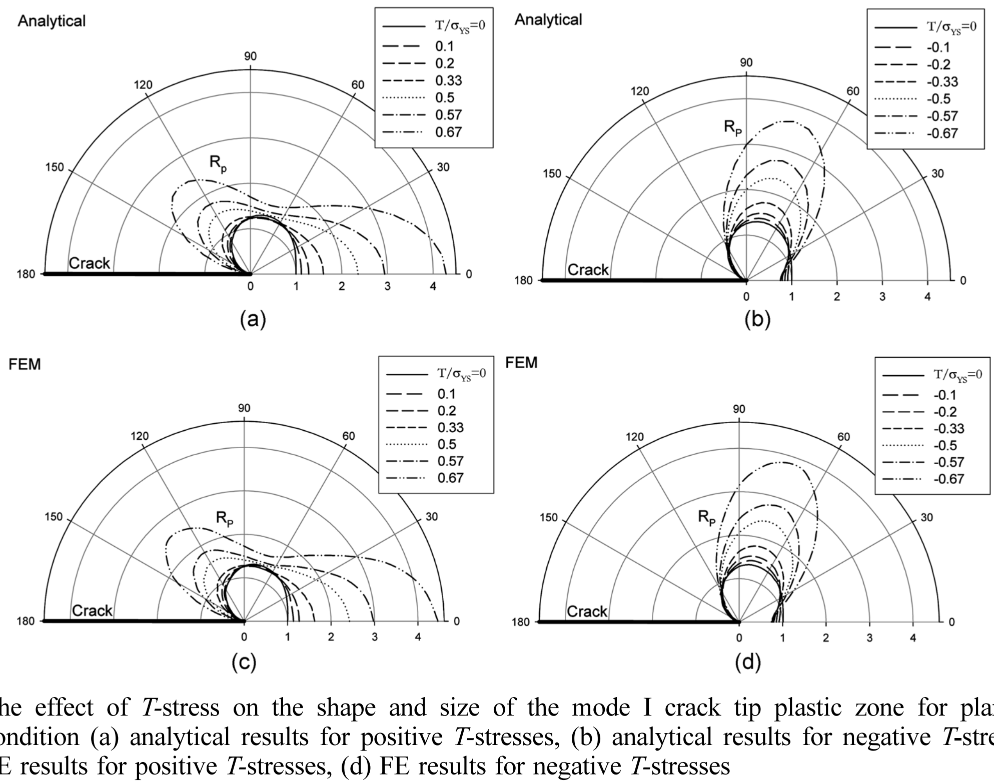

Fig. 3 The effect of *T*-stress on the shape and size of the mode I crack tip plastic zone for plane stress condition (a) analytical results for positive *T*-stresses, (b) analytical results for negative *T*-stresses, (c) FE results for positive *T*-stresses, (d) FE results for negative *T*-stresses

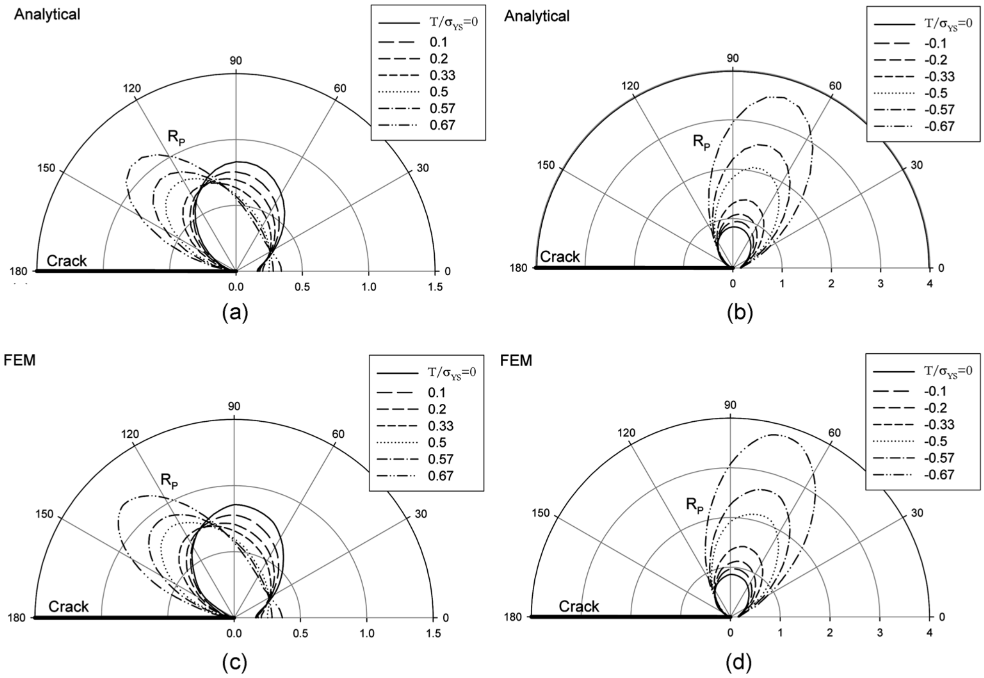

Fig. 4 The effect of *T*-stresses on the shape and size of the mode I crack tip plastic zone for plane strain condition ($\upsilon = 0.3$); (a) Analytical results for positive *T*-stresses, (b) analytical results for negative *T*-stresses, (c) FE results for positive *T*-stresses, (d) FE results for negative *T*-stresses

with respect to the crack line; only one half of the plastic zone is presented for this loading condition. Figs. 3(a) and 3(b) show the analytical radius of the plastic zone for positive *T*-stresses and negative *T*-stresses, respectively. The finite element results are also plotted in Figs. 3(c) and 3(d) for positive and negative *T*-stresses.

A comparison between Figs. 3(a) and 3(c) or Figs 3(b) and 3(d) shows that the results obtained from the analytical and finite element methods are in excellent agreement. It is seen from these figures that a *T*-stress has a considerable influence on the shape and size of the plastic zone. Both positive and negative *T*-stresses increase significantly the plastic zone size. Figs. 3(a) and 3(c) show that for the case of positive *T*-stress, the plastic zone expands as *T* increases, with the expansion in the *x* direction more significant than that in the *y* direction. For the case of negative *T*-stress, it is observed that the height of the plastic zone is significantly enlarged when the *T*-stress is decreased (Figs. 3(b) and 3(d)). Furthermore, negative *T*-stresses tilt the plastic zone forward whereas positive *T*-stresses rotate the plastic zone backwards. The effect of *T*-stress on enlarging the plastic zone is more pronounced when the specimen is at higher levels of positive or negative T/σ_{YS}.

Similar results are shown in Fig. 4 but for plane strain condition when $\upsilon = 0.3$. In the case of plane strain, the plastic zone is enlarged significantly by a negative *T*-stress. Figs. 4(a) and 4(c) show that the size of the plastic zone is first reduced a little as a positive *T*-stress increases, then it increases when T/σ_{YS} becomes larger than 0.5. These observations may partially explain why the fracture toughness of fully dense metals is significantly larger in the presence of negative *T*-stresses and insensitive to positive *T*-stresses, as suggested by Tvergaard and Hutchinson (1992, 1994) and

Chen *et al*. (2001).

As shown in Fig. 4 the normalized plastic zones turn forward remarkably for decreasing negative *T*-stresses, but change its direction backward for increasing positive *T*-stresses. A similar trend for the rotation of plastic zone shape with the sign of *T*-stress can also be seen in the finite element results presented by Betegon and Hancock (1991), O'Dowd and Shih (1991), and Shih *et al*. (1993).

4.2 Mode II crack tip plastic zone

The plastic zone boundaries normalized with respect to $1/2\pi(K_{II}/\sigma_{YS})^2$ calculated from both the proposed formulation and the finite element method are plotted in Fig. 5 for selected values of T and under plane stress condition. Fig. 6 shows similar results but for plane strain condition with $\upsilon = 0.3$. The analytical results are shown in Figs. 5(a) and 6(a) for positive *T*-stresses and in the Figs. 5(b) and 6(b) for negative *T*-stresses. Similarly, the FE Results are plotted in the Figs. 5(c) and

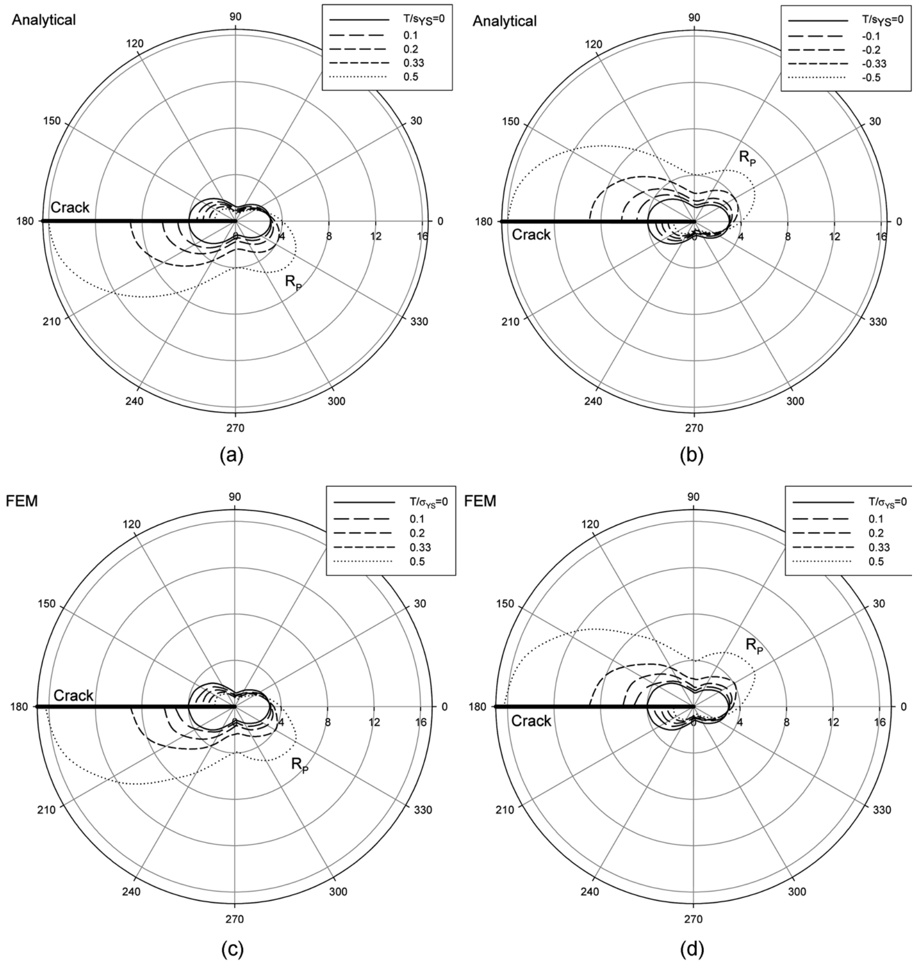

Fig. 5 The effect of *T*-stress on the shape and size of the mode II crack tip plastic zone for plane stress condition; (a) Analytical results for positive *T*-stresses, (b) Analytical results for negative *T*-stresses, (c) FE results for positive *T*-stresses, (d) FE results for negative *T*-stresses

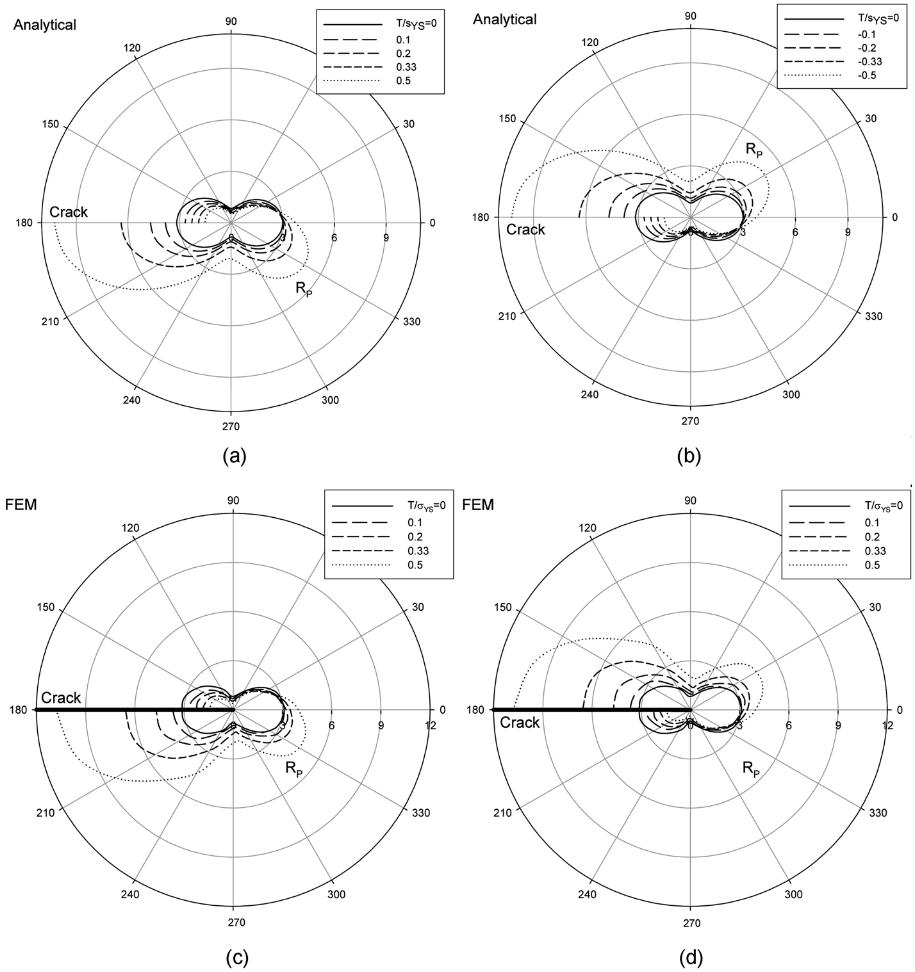

Fig. 6 The effect of T-stresses on the shape and size of the mode II crack tip plastic zone for plane strain condition ($\upsilon = 0.3$) (a) Analytical results for positive T-stresses, (b) analytical results for negative T-stresses, (c) FE results for positive T-stresses, (d) FE results for negative T-stresses

6(c) for positive T-stresses and in the Figs. 5(d) and 6(d) for negative T-stresses.

A comparison between Figs. 5(a) and 5(c), Figs. 5(b) and 5(d), Figs. 6(a) and 6(c) or Figs. 6(b) and 6(d), shows that the results obtained from the analytical and finite element methods are in excellent agreement. As expected, for T = 0 the plastic zone is symmetric with respect to the crack line. It is observed from Figs. 5 and 6 that the plastic zones are not symmetric when T is non-zero. The plastic zone consists essentially of two parts: one ahead of and one behind the crack tip. The T-stress influences both parts of the plastic zone. For the plastic zone in front of the crack tip, a positive T causes the direction of $R_{P\max}$ to rotate clockwise. The plastic zone behind the crack tip is also influenced by the T-stress such that the lower section is enlarged by a positive T whereas the upper section is contracted. It is clear from Figs. 5 and 6 that the effect of a negative T-stress on the shape and size of the plastic zone is a mirror image about the crack plane compared to that of an identical positive T-stress value.

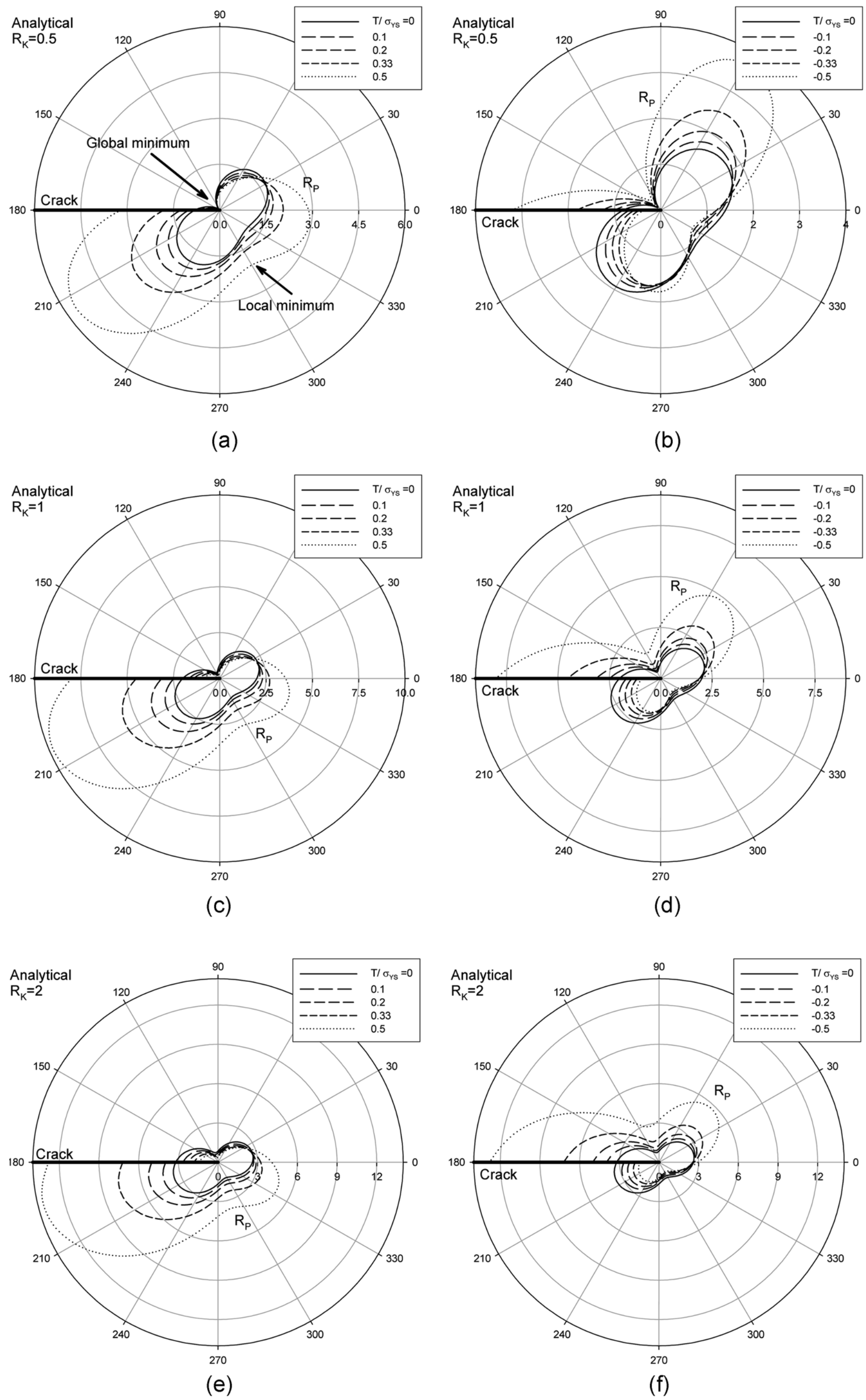

Fig. 7 The effect of *T*-stresses on the shape and size of the plastic zone under mixed mode loading for plane stress condition (a) $R_K = 0.5$, positive *T*-stresses, (b) $R_K = 0.5$, negative *T*-stresses, (c) $R_K = 1$, positive *T*-stresses, (d) $R_K = 1$, negative *T*-stresses, (e) $R_K = 2$, positive *T*-stresses, (f) $R_K = 2$, negative *T*-stresses

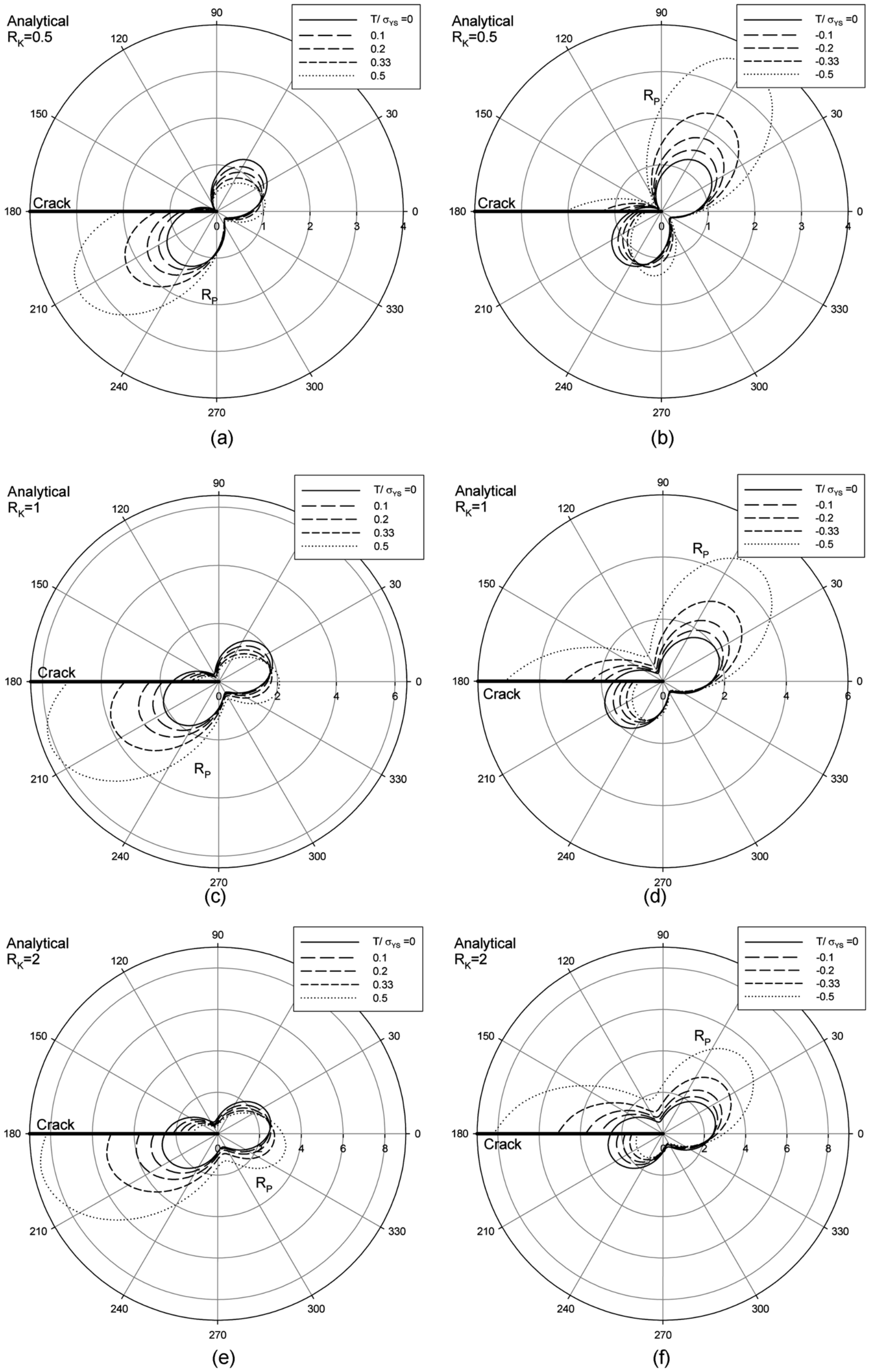

Fig. 8 The effect of *T*-stresses on the shape and size of the plastic zone under mixed mode loading for plane strain condition; (a) $R_K = 0.5$, positive *T*-stresses, (b) $R_K = 0.5$, negative *T*-stresses, (c) $R_K = 1$, positive *T*-stresses, (d) $R_K = 1$, negative *T*-stresses, (e) $R_K = 2$, positive *T*-stresses, (f) $R_K = 2$, negative *T*-stresses

4.3 Mixed mode (I+II) crack tip plastic zone

The plastic zone boundaries normalized with respect to $1/2\pi(K_{eff}/\sigma_{YS})^2$ and calculated from the proposed formulation are plotted in Fig. 7 for the selected values of T under plane stress condition and for $R_K = 0.5$, 1 and 2. For pure mode I ($R_K = 0$) and pure mode II ($R_K = \infty$), the results derived from Eq. (23) were equal to those obtained from Eqs. (13a) and (13b), respectively. Figs. 7(a), 7(c) and 7(e) show the analytical radius of the plastic zone for positive T-stresses, while in the Figs. 7(b), 7(d) and 7(f) the analytical radius of the plastic zone is plotted for negative T-stresses. It should be noted that the analytical findings were again compared with the finite element results of a boundary layer model and a very good agreement was observed between these results. However, for the sake of brevity the finite element results are not repeated here.

It can be seen from Fig. 7 that, under mixed mode loading, an increase in positive T-stress causes the upper part of the plastic zone (relative to the crack line) to become smaller and the lower part to expand along the crack face. Moreover, there are two different directions for which the plastic zone size exhibits local maxima: one in front section of the crack and one in the rear section of the crack. A positive T causes the direction of $R_{P\max}$ in the front section of crack to rotate clockwise. This rotation increases for larger values of T/σ_{YS}. According to Fig. (7) for positive T-stresses when R_K is increased, the upper part of the plastic zone vanishes compared to the lower lobe of the plastic zone. The opposite of the effects described above for positive T-stresses occurs for negative T-stresses (see Figs. 7(b), 7(d) and 7(f)). Moreover, it is seen that for higher values of R_K, the plastic zone corresponding to a fixed T/σ_{YS} extends both ahead of the crack tip as well as along the crack face.

Similar results are shown in Fig. 8 but for plane strain condition when $\upsilon = 0.3$. A comparison between Figs. 7 and 8 shows that the effects of T-stress on the normalized plastic zone are qualitatively similar for both plane stress and plane strain conditions, although certain differences exist quantitatively.

As shown in Fig. 7(a), for a given loading configuration, two minima can be identified along the elastic-plastic boundary. One is a local minimum and the other is a global minimum. The variations of the local minimum radius for different T-stresses are shown in Figs. 9(a) and 10(a) for plane

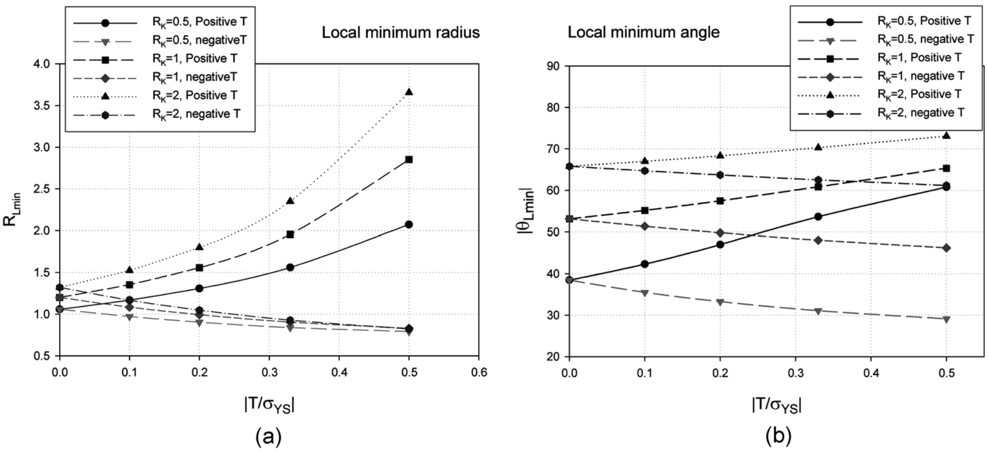

Fig. 9 (a) Radius of local minimum in the plastic zone for plane stress condition, (b) its corresponding angle

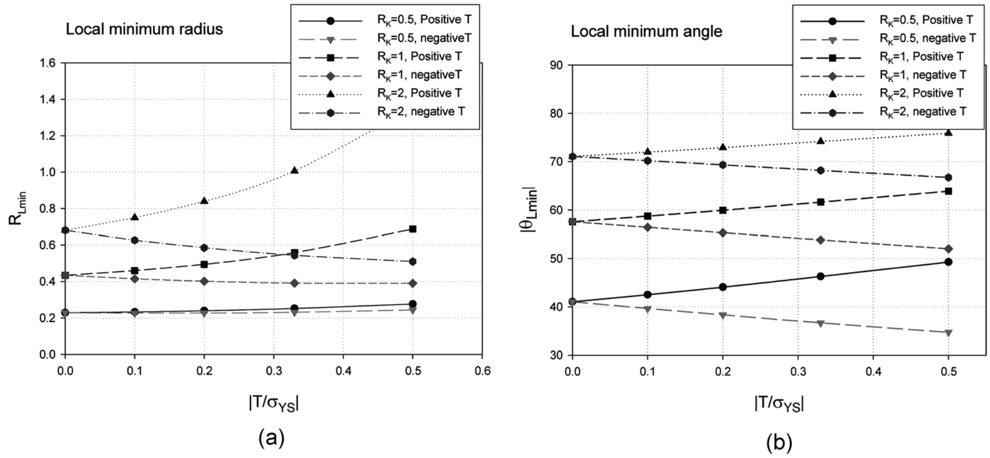

Fig. 10 (a) Radius of local minimum in the plastic zone for plane strain condition, (b) its corresponding angle

stress and plane strain conditions, respectively. The angle corresponding to this minimum radius is plotted versus $|T/\sigma_{YS}|$ in Figs. 9(b) and 10(b) for plane stress and plane strain conditions.

4.4 Fracture initiation angle

Many researchers in the field of fracture mechanics have shown an interest in studying the fracture initiation angle under mixed mode loading. For a reliable prediction of the crack propagation path, a suitable criterion for defining the fracture initiation angle is a vital issue. The study of fracture initiation angle is also very important in the design and implementation of techniques for arresting cracks. Several criteria have been proposed for predicting the fracture initiation angle in cracked components under mixed mode loading (e.g., Erdogan and Sih 1963, Sih 1973, Sih 1974, Theocaris and Andrianopoulos 1982, Theocaris *et al*. 1983, Ukadgaonker and Awasare 1995, Kong *et al*. 1995, Khan and Khraisheh 2000, Smith *et al*. 2001, Alshoaibi 2010). Recently, Khan and Khraisheh (2000) presented a detailed review of mixed mode I-II fracture based on explicit fracture prediction theories. These criteria are often proposed on the basis of a mechanical parameter (like stress, strain, energy and etc.) and evaluated by using appropriate test specimens.

In general, it is established that the nature of the crack tip plastic zone has a major effect in the process of crack extension and propagation. Khan and Khraisheh (2004) investigated the role of the plastic zone shape in determining the initial crack extension and then based on the characteristics of the plastic zone presented a new criterion called the minimum plastic zone radius theory or the R-criterion. They suggested that the fracture initiation angles follow either the local or the global minimum of the elastic-plastic boundary depending on the resultant stresses at the crack face. The plastic zone presents a highly strained area through which the crack tip has to propagate to reach the elastically loaded material outside the plastic zone. The crack can be assumed to follow the "easiest" path or the shortest distance to the outside material. The shortest distance from the crack tip to the elastic-plastic boundary represents the minimum plastic work needed to create the crack surfaces or the path that requires the minimum fracture energy, as explained in Khan and Khraisheh (2004). Therefore, the *R*-criterion can be defined on the assumption that the crack tip will follow a path towards the minimum radius of the plastic zone (Khan and Khraisheh 2004). The minimum plastic zone radius theory for the fracture initiation angle was also extended to surface cracks under mixed mode loading by Bian and Kim (2004). According to this criterion, the fracture initiation angle can be determined mathematically as

$$\frac{\partial R_P}{\partial \theta} = 0, \quad \frac{\partial^2 R_P}{\partial \theta^2} > 0 \tag{26}$$

Meanwhile, based on the tangential stress as a critical parameter for crack initiation, Erdogan and Sih (1963) proposed a criterion called the maximum tangential stress (MTS) criterion for the fracture initiation under mixed mode loading. This criterion states that the onset of crack extension takes place in the direction of maximum tangential stress along a constant radius around the crack tip. Smith *et al*. (2001) later presented a generalized MTS criterion for mixed mode brittle fracture. The generalized criterion takes into account the effects of both the singular terms and the T term in the tangential stress around the crack tip. According to Smith *et al*. (2001), the initial direction of crack propagation and the mixed mode fracture toughness of a cracked specimen depend on the magnitude and the sign of T-stress. They also found that a positive T increases the initial angle of crack propagation whereas a negative T reduces the fracture initiation angle. These results were also validated by using extensive experimental results, e.g. Ayatollahi *et al*. (2006) and Ayatollahi and Aliha (2009).

Similar to the modification suggested by Smith *et al*. (2001) for the MTS criterion, the conventional R-criterion is modified here to take into account the effect of T-stress. According to Figs. 9 and 10 it is clear that a negative T-stress causes the local minimum of the plastic zone to rotate in the counterclockwise direction and the fracture initiation angle decreases, while a positive T-stress causes the local minimum of the plastic zone to rotate in the clockwise direction and hence increases the fracture initiation angle. Therefore, in order to estimate the initial direction of crack propagation the R-criterion can be modified by using the formulation presented in this paper for the boundary of plastic zone. In general, the effect of T-stress on the fracture initiation angle described above by the R-criterion is similar to what Smith *et al*. (2001) found.

In order to assess the modified R-criterion by experimental results, the reported values of fracture initiation angle for PMMA (Ayatollahi *et al*. 2006) are used here. The tests were conducted on a semi-circular bend (SCB) specimen in which the T-stress is of a significant value. As shown in Fig. 11, the SCB specimen is a semi-circular disc subjected to three point bending and containing an

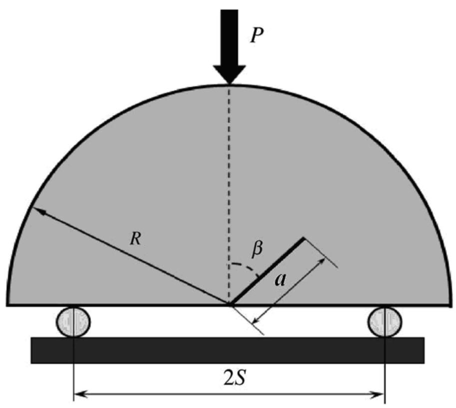

Fig. 11 Cracked semi-circular bend (SCB) specimen (Ayatollahi *et al*. 2006)

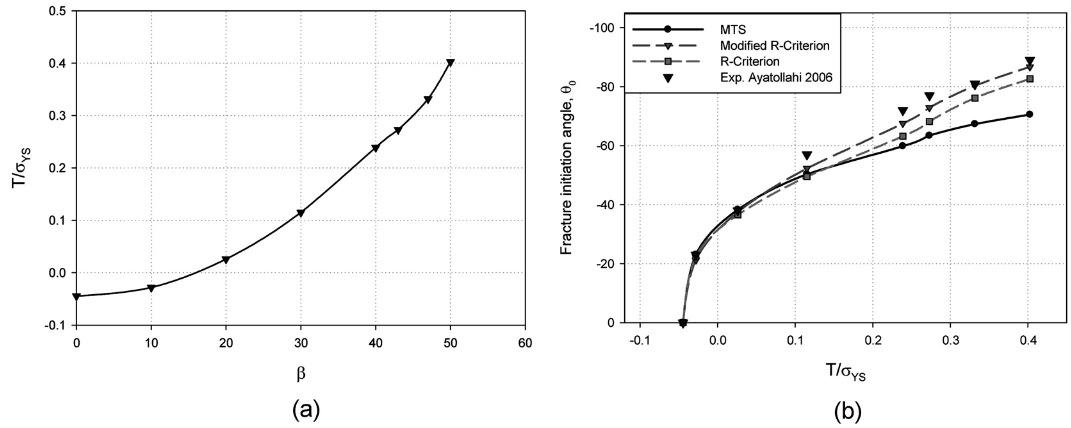

Fig. 12 (a) Variations of the normalized *T*-stress (T/σ_{YS}) versus the crack angle β, (b) crack initiation angle, θ_0, versus normalized *T*-stress (T/σ_{YS})

edge crack of length a. The crack makes an angle β relative to the vertical direction. The radius of semi-circular specimen R, the crack length ratio a/R and the loading distance ratio S/R were 50 mm, 0.3 and 0.43, respectively (Ayatollahi *et al*. 2006). The material properties of $\sigma_{YS} = 70$ MPa and $\nu = 0.38$ were used for PMMA based on Gómez *et al*. (2005) and the numerical values of *T*-stress versus angle β, were taken from Ayatollahi *et al*. 2006. Considering the relatively low thickness/diameter ratio in the tested specimens, a state of plane stress was used in our analyses.

Fig. 12(a) displays the variations of the normalized *T*-stress (T/σ_{YS}) with the crack angle β for the SCB specimens (Ayatollahi *et al*. 2006). According to this figure, by moving from pure mode I towards pure mode II, the *T*-stress becomes larger. Fig. 12(b) shows the experimentally observed fracture initiation angles together the theoretical values predicted by the MTS, *R* and modified *R* criteria. It is seen that the results estimated by the modified *R*-criterion are in better agreement with the experimental results compared to the results of the MTS and *R* criteria.

It is finally reminded that the closed form solutions presented in this paper were derived within the framework of linear elastic fracture mechanics. Thus, the results are valid only for small to moderate scale yielding where elastic analysis provides an acceptable estimate of the crack tip stress field. For large scale yielding, the shape and size of plastic zone should be determined using the concepts of elastic-plastic fracture mechanics.

5. Conclusions

The effects of *T*-stress on the shape and size of the plastic zone around the crack tip were determined for small scale yielding and under mode I, mode II and mixed mode loadings and for both plane stress and plane strain conditions. Closed form formulations for the normalized radius of the plastic zone were presented that could be used for different loading conditions. The following can be concluded:

1. The analytical formulation allowed us to recognize a well-defined correlation between the *T*-stress and the plastic zone boundary. The results obtained by the proposed analytical formulation show a very good agreement with those obtained from the finite element analysis.

2. Both the analytical and the FE results indicate that the *T*-stress has a considerable influence on the size and shape of the plastic zone.

3. In the case of plane stress conditions and under pure mode I loading, the results show that both positive and negative *T*-stresses increase the plastic zone size significantly. It has been observed that the plastic zone expands as positive *T*-stress increases, with the expansion in the x direction more significant than that in the y direction. Moreover, the height of the plastic zone is significantly enlarged with a decrease in the negative *T*-stress. In the case of plane strain condition, the plastic zone is enlarged significantly by a negative *T*-stress but is changed slightly by a positive *T*-stress.

4. Under pure mode II loading conditions, the results indicate that for the plastic zone in front of the crack tip, a positive T causes the direction of $R_{P\max}$ to rotate clockwise. The plastic zone behind the crack tip is also influenced by the *T*-stress such that the lower section is enlarged by a positive T whereas the upper section is contracted. The effect of a negative *T*-stress on the shape and size of the plastic zone is a mirror image about the crack plane compared to that of an identical positive *T*-stress value.

5. Under mixed mode loading, it was observed that an increase in positive *T*-stress causes the upper part of the plastic zone to become smaller and the lower part to expand along the crack face. A positive T causes the direction of $R_{P\max}$ in front of the crack tip to rotate clockwise. Opposite to the effects described for positive *T*-stresses occurs for negative *T*-stresses.

6. Under predominantly mode I loading, the effect of a negative *T*-stress on the size of the plastic zone is more significant than that of a positive *T*-stress. However, when the mode II portion of loading is dominated, the size of the plastic zone is almost the same for both positive and negative *T*-stresses.

7. A mixed mode fracture theory called the *R*-criterion was modified by taking into account the effect of *T*-stress on the shape and size of the plastic zone. The modified criterion could provide good predictions for the experimentally observed fracture initiation angles reported in an earlier paper.

References

Al-Ani, A.M. and Hancock, J.W. (1991), "J-dominance of short cracks in tension and bending", *J. Mech. Phys. Solids*, **39**, 23-43.

Alshoaibi, A.M. (2010) "Finite element procedures for the numerical simulation of fatigue crack propagation under mixed mode loading", *Struct. Eng. Mech.*, **35**(3).

Anderson, T.L. (1995), *Fracture Mechanics: Fundamentals and Applications*, Second Edition, CRC Press.

Arun Roy, Y. and Narasimhan, R. (1997), "J-dominance in mixed mode ductile fracture specimens", *Int. J. Fract.*, **88**, 259-279.

Ayatollahi, M.R. and Aliha, M.R.M. (2009), "Mixed mode fracture in soda lime glass analyzed by using the generalized MTS criterion", *Int. J. Solids Struct.*, **46**, 311-321.

Ayatollahi, M.R., Aliha, M.R.M. and Hassani, M.M. (2006), "Mixed mode brittle fracture in PMMA-An experimental study using SCB specimens", *Mater. Sci. Eng.*, **417**, 348-356.

Ayatollahi, M.R., Pavier, M.J. and Smith, D.J. (1996), "On mixed mode loading of a single edge notched specimen", *Int. J. Fract.*, **82**, R61-R66.

Ayatollahi, M.R., Pavier, M.J. and Smith, D.J. (1998), "Determination of T-stress from finite element analysis for mode I and mixed mode I/II loading", *Int. J. Fract.*, **91**, 283-298.

Ayatollahi, M.R., Pavier, M.J. and Smith, D.J. (2002a), "A New Specimen for Mode II Fracture tests", ECF14, Poland, **1**, 161-168.

Ayatollahi, M.R., Pavier, M.J. and Smith, D.J. (2002b), "Crack-tip constraint in mode II deformation", *Int. J. Fract.*, **113**, 153-173.

Banks, T.M. and Garlick, A. (1984), "The form of crack tip plastic zones", *Eng. Fract. Mech.*, **19**, 571-581.

Benrahou, K.H., Benguediab, M., Belhouari, M., Nait-Abdelaziz, M. and Imad, A. (2007), "Estimation of the plastic zone by finite element method under mixed mode (I and II) loading", *Comput. Mater. Sci.*, **38**, 595-601.

Betegon, C. and Hancock, J.W. (1991), "Two-parameter characterization of elastic-plastic crack-tip fields", *J. Appl. Mech.*, **58**, 104-110.

Bian, L.C. (2007), "Material plasticity dependence of mixed mode fatigue crack growth in commonly used engineering materials", *Int. J. Solids Struct.*, **44**, 8440-8456.

Bian, L.C. and Kim, K.S. (2004), "The minimum plastic zone radius criterion for crack initiation direction applied to surface cracks and through-cracks under mixed mode loading", *Int. J. Fatigue*, **26**, 1169-1178.

Bilby, B.A., Carden, G.E., Goldthorpe, M.R. and Howard, I.C. (1986), *Size Effect in Fracture*, Mechanical Engineering Publications, London.

Broek, D. (1982), *Elementary Engineering Fracture Mechanics*, Martinus Nijhoff Publishers.

Chen, C., Fleck, N.A. and Lu, T.J. (2001), "The mode I crack growth resistance of metallic foams", *J. Mech. Phys. Solids*, **49**, 231-259.

Du, Z.Z. and Hancock, J.W. (1991), "The effect of non-singular stresses on crack tip constraint", *J. Mech. Phys. Solids*, **39**, 555-567.

Edmunds, T.M. and Willis, J.R. (1977), "Matched asymptotic expansions in nonlinear fracture mechanics-III. In-plane loading of an elastic perfectly-plastic symmetric specimen", *J. Mech. Phys. Solids*, **25**, 423-455.

Erdogan, F. and Sih, G.C. (1963), "On the crack extension in plates under plane loading and transverse shear", *J. Basic Eng.*, **85**, 519-525.

Fett, T. (2001), "Stress intensity factors and T-stress for internally cracked circular disks under various boundary conditions", *Eng. Fract. Mech.*, **68**, 1119-1136.

Gómez, F.J., Elices, M. and Planas J. (2005), "The cohesive crack concept: application to PMMA at 60C", *Eng. Fract. Mech.*, **72**, 1268-1285.

Haefele, P.M. and Lee, J.D. (1995), "The constant stress term", *Eng. Fract. Mech.*, **50**, 869-882.

Harmain, G.A. and Provan, J.W. (1997), "Fatigue crack-tip plasticity revisited — The issue of shape addressed", *Theor. Appl. Fract. Mec.*, **26**, 63-79.

Irwin, G.R. (1948), *Fracture Dynamics. Fracturing of Metals*, ASM, Cleveland, Chio.

Jing, P.H. and Khraishi, T. (2004), "Analytical solutions for crack tip plastic zone shape using the von mises and tresca yield criteria: Effects of crack mode and stress condition", *J. Mech.*, **20**, 199-210.

Jing, P., Khraishi, T. and Gorbatikh, L. (2003), "Closed-form solutions for the mode II crack tip plastic zone shape", *Int. J. Fract.*, **122**, L137-142.

Khan, S.M.A. and Khraisheh, K. (2004), "A new criterion for mixed mode fracture initiation based on the crack tip plastic core region", *Int. J. Plast.*, **20**, 55-84.

Khan, S.M.A. and Khraisheh, M.K. (2000), "Analysis of mixed mode crack initiation angles under various loading conditions", *Eng. Fract. Mech.*, **67**, 397-419.

Kim, Y., Zhu, X.K. and Chao, Y.J. (2001), "Quantification of constraint on elastic plastic 3D crack front by the J-A2 three-term solution", *Eng. Fract. Mech.*, **68**, 895-914.

Kong, X.M., Schluter, N. and Dahl, W. (1995), "Effect of triaxial stress on mixed-mode fracture", *Eng. Fract. Mech.*, **52**, 379-388.

Larsson, S.G. and Carlsson, A.J. (1973), "Influence of non-singular stress and specimen geometry on small-scale yielding at each tip in elastic-plastic materials", *J. Mech. Phys. Solids*, **21**, 263-277.

Mishra, S.C. and Parida, B.K. (1985), "Determination of the size of crack-tip plastic zone in a thin sheet under uniaxial loading", *Eng. Fract. Mech.*, **22**, 351-357.

O'Dowd, N.P. and Shih, C.F. (1991), "Family of crack-tip fields characterized by a triaxiality parameter-I. Structure of fields", *J. Mech. Phys. Solids*, **39**, 989-1015.

Rice, J.R. (1968), *A Mathematical Theory of Fracture, In: Fracture*, Academic press, New York.

Rice, J.R. (1974), "Limitations to the small scale yielding for crack-tip plasticity", *J. Mech. Phys. Solids*, **22**, 17-26.

Shih, C.F., O'Dowd, P.N. and Kirt, M.T. (1993), "A framework for quantifying crack tip constraint", *ASTM STP*, **1171**, 2-20.

Sih, G.C. (1973), "Some basic problems in fracture mechanics and new concepts", *Eng. Fract. Mech.*, **5**, 365-377.

Sih, G.C. (1974), "Strain-energy-density factor applied to mixed mode crack problems", *Int. J. Fract.*, **10**, 305-321.

Smith, D.J., Ayatollahi, M.R. and Pavier, M.J. (2001), "The role of T-stress in brittle fracture for linear elastic materials under mixed-mode loading", *Fatigue Fract. Eng. Mater. Struct.*, **24**, 137-150.

Theocaris, P.S. and Andrianopoulos, N.P. (1982), "The Mises elastic-plastic boundary as the core region in fracture criteria", *Eng. Fract. Mech.*, **16**, 425-432.

Theocaris, P.S., Kardomateas, G.A. and Andrianopoulos, N.P. (1983), "Experimental study of the T-criterion in ductile fracture", *Eng. Fract. Mech.*, **17**, 439-447.

Tvergaard, V. and Hutchinson, J.W. (1992), "The relation between crack growth resistance and fracture process parameters in elastic-plastic solids", *J. Mech. Phys. Solids*, **40**, 1377-1397.

Tvergaard, V. and Hutchinson, J.W. (1994), "Effect of T-stress on mode-I crack growth resistance in a ductile solid", *Int. J. Solids Struct.*, **31**, 823-833.

Ukadgaonker, V.G. and Awasare, P.J. (1995), "A new criterion for fracture initiation", *Eng. Fract. Mech.*, **51**, 265-274.

Wang, Y.Y. (1993), "On the two-parameter characterization of elastic-plastic front field in surface crack cracked plates", *ASTM Special Technical Publication*, **1171**, 120-138.

Williams, M.L. (1957), "Stress singularities resulting from various boundary conditions insingular corners of plates in extension", *J. Appl. Mech.*, **19**, 526-528.

Yuan, H. and Broeks, W. (1998), "Quantification of constraint effects in elastic plastic crack front field", *J. Mech. Phys. Solids*, **46**, 219-241.

Zhang, J.P. and Venugopalan, D. (1987), "Effects of notch radius and anisotropy on the crack tip plastic zone", *Eng. Fract. Mech.*, **26**, 913-925.

Notations

K	: stress intensity factor
I, II, III	: subscripts denoting mode of loading
K_{eff}	: effective stress intensity factor
x, y	: cartesian coordinates at the crack tip
X, Y	: normalized Cartesian coordinate at the crack tip
r, θ	: polar coordinates at the crack tip
R, θ	: normalized Polar coordinates at the crack tip
σ_x, σ_y, σ_{xy}	: stresses at the crack tip
σ_{ij}	: stress tensor
σ_{eff}	: effective stress
υ	: Poisson's ratio
b	: ratio of T-stress to the yield stress
r_P	: radius of the plastic zone
R_P	: normalized radius of the plastic zone
R_0	: boundary layer model radius
$R_{P\max}$	: maximum radius of the normalized plastic zone
R_K	: ratio of the K_{II} to K_I
a	: crack length
σ_{YS}	: yield stress
E	: Young's modulus
T	: T-stress terms (T-stresses)
Y	: geometry factor
u_1, u_2, u_3	: components of the displacement vector
$f_{ij}(\theta)$, $g_{ij}(\theta)$, $h_{ij}(\theta)$	: universal functions of θ
$f_i(\theta)$	: angular functions in Williams' series expansion
Q	: unknown functions
$F(\theta, \upsilon, Y)$	: unknown functions
G	: unknown functions